FIRE PERFORMANCE OF CFRP STRENGTHENED AND INSULATED SQUARE HOLLOW SECTION COLUMNS

MOHAMED IMRAN[1] and MAHEN MAHENDRAN[1]

[1]*School of Civil Engineering, Queensland University of Technology, Brisbane, Australia.*
E-mail: m.imran@qut.edu.au; m.mahendran@qut.edu.au

In this study, fire performance of CFRP strengthened short Square Hollow Section (SHS) columns with and without external insulation was investigated using finite element modelling. CFRP strengthened SHS columns were tested under uniform elevated temperature and standard fire test conditions. These tests showed a significant reduction in capacity and fire resistance and thus the need for protecting them with external insulation. Steady state finite element models of CFRP strengthened SHS columns under uniform temperature exposure were developed and validated, and were used to determine the load ratio versus critical temperature curves for varying SHS sizes and CFRP configurations. Transient state finite element models of CFRP strengthened and externally insulated SHS steel columns under standard fire conditions were then developed and validated using fire test results. Two external insulation materials (spray applied CAFCO300 and intumescent paint) of varying thicknesses were considered. Finally, fire resistance ratings (FRR) of CFRP strengthened and externally insulated SHS columns were determined based on the time-temperature curves obtained from heat transfer analyses, and the load ratio versus critical failure temperature curves from steady state finite element analyses. FRR results showed that both types of insulation provided satisfactory FRRs for most columns.

Keywords: Steel tubular columns, CFRP strengthening, Insulation, Fire Performance.

1 Introduction

CFRP strengthened steel columns have significantly enhanced axial compression capacities as shown by recent studies (Shaat and Fam 2006, Bambach et al. 2009). However, they suffer from reduced fire resistance because CFRP composites soften at much lower temperatures (65-120°C). The adhesives (an epoxy) used have a low glass transition temperature in the above range. Such concern regarding CFRP composites has hampered the use of CFRP in strengthening steel columns, which require specific fire resistance ratings (FRR). Hence detailed experimental and numerical studies were conducted at the Queensland University of Technology to investigate the fire performance of CFRP strengthened steel columns (Imran 2018).

A series of tests on short CFRP strengthened SHS (Square Hollow Section) steel columns was first conducted under steady state conditions, where the columns were exposed to a uniform elevated temperature and then loaded in compression to failure. Tests showed that the axial compression capacity reduced significantly when temperatures exceeded the glass transition temperature of the adhesive, and the CFRP became ineffective beyond 225°C. Hence the use of an external insulation system was recommended to protect the CFRP strengthened steel columns. A series of standard fire tests was then conducted on CFRP strengthened SHS columns externally insulated with 30 mm thick Vermiculite and Gypsum based spray applied insulation, CAFCO300 (Figure 1), which showed the effectiveness of external insulation (>60 min FRR).

Proceedings of the 17th International Symposium on Tubular Structures.
Editors: X.D. Qian and Y.S. Choo

Published by Research Publishing, Singapore.
ISBN: 978-981-11-0745-0; doi:10.3850/978-981-11-0745-0_105-cd

CFRP strengthened and insulated reinforced concrete column tests also showed the effectiveness of external insulation (Kodur et al. 2006). Grade 350 100×100×2mm SHS columns of 300 mm height were used in the tests with 1T1L and 2T2L CFRP configurations in the first and second test series, respectively (1T1L: one layer each in transverse and longitudinal directions).

Figure 1. CFRP Strengthened and Externally Insulated SHS Columns

Finite element (FE) modelling was then used to study the behaviour of CFRP strengthened short steel tubular columns (SHS) with and without external insulation (Figure 1) subject to local buckling failures in fire. Steady state FE models of CFRP strengthened SHS columns under uniform temperature conditions were developed and validated, and were used to determine the load ratio-critical temperature curves for varying SHS sizes and CFRP configurations. Transient state FE models of CFRP strengthened and externally insulated SHS columns under standard fire conditions were also developed and validated using fire test results. Two insulation materials (CAFCO300 and intumescent paint) were used. Using the load ratio-critical failure temperature curves from steady state FEA and the heat transfer analysis results of time-temperature curves, fire resistance ratings (FRR) of CFRP strengthened and externally insulated SHS columns were determined. This paper presents the details of this numerical study and the results.

2 Finite Element Modelling

3D FE models of experimentally tested SHS columns were developed using ABAQUS/CAE software. They included three parts of SHS steel column, adhesive and CFRP (Figure 2), with 4 mm × 4 mm mesh. The contact between each layer was modelled by sharing the nodes with the base surface. Adhesive was modelled between the steel column and the first CFRP layer.

2.1 Material properties, element types and analysis methods

The steel column was modelled as an elastic-plastic material with strain hardening. The required elevated temperature stress-strain characteristics were determined from Imran et al. (2018) and the measured ambient temperature mechanical properties in Table 1. The adhesive layer between steel and CFRP was modelled using coupled cohesive zone model based on traction separation law, where the initial response is assumed to be linear until damage initiation (De Lorenzis et al. 2013) based on mixed mode failure criteria. Damage is initiated when the function reaches a value of one and damage evolution initiates. The damage evolution phenomenon was modelled using energy based linear softening approach in ABAQUS using Benzeggah-Kenane fracture energy based mixed mode law. The required maximum fracture energies, which cause failures in normal and shear directions, were obtained from Alam et al. (2015) and the ambient temperature material properties of adhesive used here are given in Table 1.

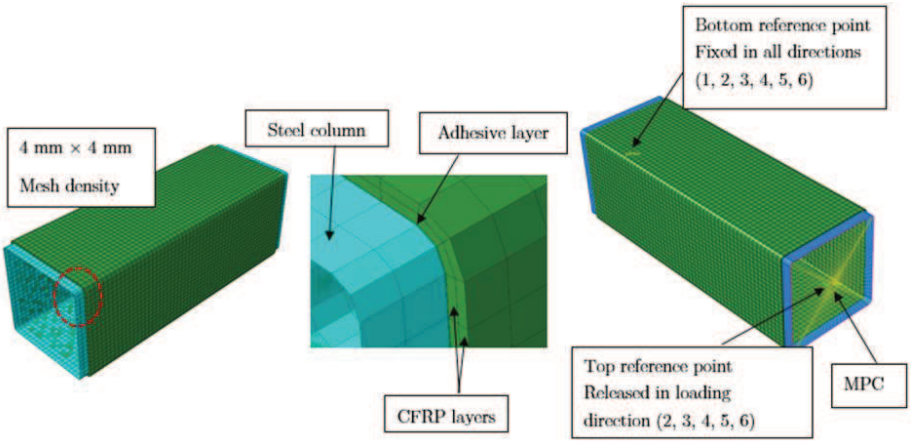

Figure 2. Finite Element Model

Table 1. Ambient Temperature Material Properties

Steel		Adhesive		CFRP	
Parameter	Value	Parameter	Value	Parameter	Value
Elastic modulus	207 GPa	E_a	1.995 GPa	E_{1C}	88.6 GPa
Yield strength	359 MPa	σ_{max}	49.3 MPa	E_{2C}	22.2 GPa
Ult.strength	407 MPa	τ_{max}	44.4 MPa	T^L	903 MPa
Poisson's ratio	0.3	k_{nn}	$1.995x10^3$ N/m^3	G_{ft}	91600 N/m
		$k_{ss} = k_{tt}$	$1.0x10^3$ N/m^3	G_{fc}	79900 N/m
		G_I	3900 N/m	G_{mt}	220 N/m
		G_{II}	11000 N/m	G_{mc}	1100 N/m

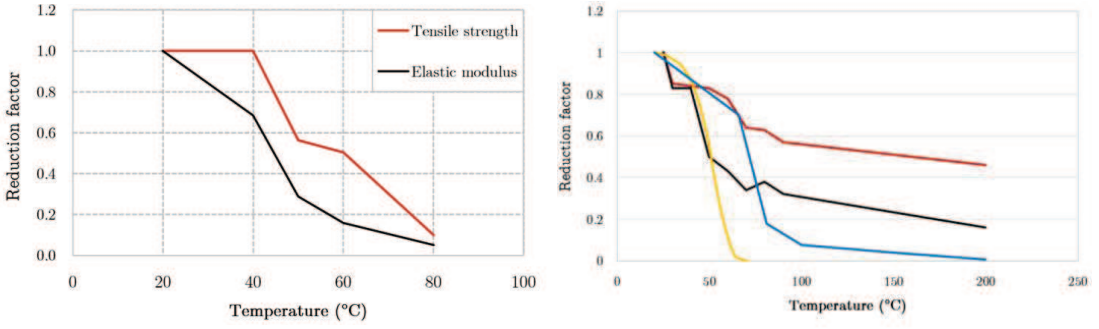

Figure 3. Mechanical property reduction factors of adhesive and CFRP

Elevated temperature mechanical properties of adhesives were obtained by using the tensile strength (σ_{max}) and elastic modulus (E_a) reduction factors of the adhesive in Ferrier et al. (2016) and the ambient temperature mechanical properties in Table 1. Figure 3 shows severe reductions in mechanical properties at elevated temperatures. Since CFRPs were found to be ineffective at 225°C (Imran 2018), both properties were taken as zero at 225°C. Elevated temperature variations of k_{nn}, k_{ss} and k_{tt} (elastic stiffness in normal and shear directions), and τ_{max} (shear strength) were determined based on these reduction factors using the ambient temperature material properties. Elevated temperature G_I and G_{II} (maximum fracture energies in normal and shear directions) are primarily dependent on the tensile and shear strengths of the adhesive at

any temperature and thus these fracture energies were obtained based on the elevated temperature tensile and shear strength reduction factors, respectively (Teng et al. 2015). Table 1 shows the average tensile strength (T^L) and elastic modulus (E_{1C}) obtained from tensile tests.

In the FE model, the CFRP composite was modelled using lamina type elastic material and the elastic-brittle damage behaviour of CFRPs was simulated using Hashin failure criteria (Hashin 1980). Four CFRP failure modes were considered, fibre rupture in tension, fibre buckling in compression, matrix cracking under transverse tension and shearing, and matrix crushing under transverse compression and shearing. Damage evolution initiates when the damage criterion is met for a given failure mode and the damage is achieved when the energy dissipated is equal to the critical fracture energy of a given failure mode. Hence, the critical fracture energies for each failure mode are required in the FE model. The fracture energies of Faggiani and Falzon (2010) agreed well with the test results of this study and hence they were used. Table 1 provides the fracture energies, where *G* refers to the fracture energy and subscripts *f, m, t* and *c* refer to fibre, matrix, tension and compression, respectively. The compressive strength (C^L) of CFRP varies from 9 to 60% of the tensile strength (Nunes et al. 2016) and hence the longitudinal compressive strength of CFRP was assumed as 20% of the tensile strength. The transverse tensile/compressive and longitudinal/transverse shear strengths were assumed to be 10% of the tensile strength (Faggiani and Falzon 2010). Poisson's ratio was taken as 0.33.

The elevated temperature tensile and shear strengths of CFRP were determined using Cree et al.'s (2015) reduction factors. Elastic modulus reduction factors were taken similar to Nguyen et al. (2011), but its sudden reduction was shifted to incorporate the difference in glass transition temperature (42 vs 66°C in this study) (Figure 3). Associated elevated temperature critical fracture energies were determined using tensile strength reduction factors.

In the steady state FE analysis, the column temperature was increased to the target temperature (20, 66, 81, 100, 150, 200 225°C) and then the load was increased until failure. SHS steel column, CFRP and adhesive layers were modelled with S4R shell elements, SC8R, 8-node quadrilateral shell elements, and 8-node 3-D cohesive element (COH3D8), respectively. After assigning the elevated temperature material properties to all three parts, elastic buckling and nonlinear analyses were conducted to determine the critical buckling mode and the failure load.

In the transient state FE analysis, heat transfer analysis was conducted first to obtain the time-temperature curves of CFRP and steel surfaces based on the measured thermal properties. Steel column, CFRP and adhesive layers were modelled using 4-node thermally coupled shell elements (S4RT), 8-node thermally coupled quadrilateral shell elements (SC8RT) and 8-node 3D cohesive element (COH3D8), respectively. The time-temperature curves agreed well with experimental results from Imran (2018) and both sets of results showed that external insulation delayed the temperature rise on CFRP and steel surfaces. The time-temperature curves of CFRP and steel surfaces were then used in a structural analysis to determine the failure time.

2.2 *Validation of FE models*

Steady state FEA results of failure loads and local buckling failure modes agree well with test results (Table 2 and Figure 4), where SS-100 means steady state and 100 ℃. Similarly, transient state FEA results agree well with standard fire (SF) test results of CFRP strengthened SF-0.2 and SF-0.3 columns with 30 mm CAFCO300 external insulation (Figure 4). SF-0.2 column under 0.2 load ratio failed at 61 min compared to FEA prediction of 55 min. For SF-0.3 column, these failure times were 50 and 52 min. Differences in axial displacement were possibly due to steel expansion. These comparisons show that the developed steady and transient state FE models are able to predict the capacity and failure time of CFRP strengthened SHS columns in fire.

Table 2. Comparison of failure loads from tests and FEA

Test Column	Failure load (kN)		FEA/Test failure load
	Test	FEA	
SS-20	281.6	291.3	1.03
SS-66	263.4	274.1	1.04
SS-81	228.1	231.8	1.02
SS-100	197.4	205.4	1.04
SS-150	180.1	188.3	1.05
SS-200	167.5	165.9	0.99
SS-225	164.5	162.6	0.99

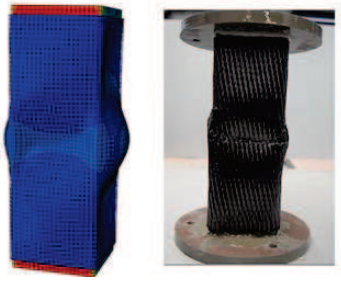

SS-100 Column

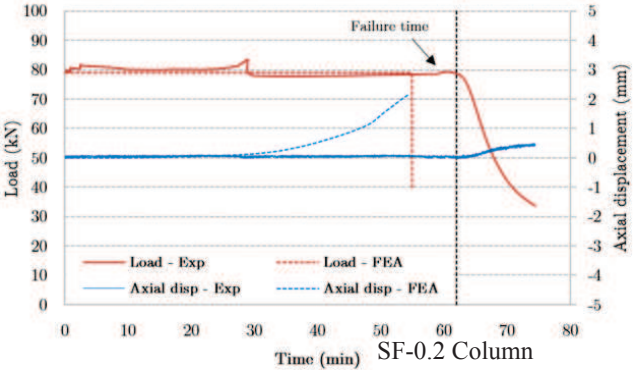

SF-0.2 Column

Figure 4. Comparison of results from tests and FEA.

3 Parametric Study

In the parametric study, the validated steady state FE models were used to develop the results of axial compression capacities for four SHS sections (100×100×2, 200×200×2, 200×200×5 and 350×350×8), two steel grades (Grade 350 and 450), four CFRP configurations (1T, 1L, 1T1L and 2T2L) and temperatures (20, 66, 81, 100, 150 and 200°C). The compression capacity beyond 225°C was taken as that of the unstrengthened column since CFRP becomes ineffective.

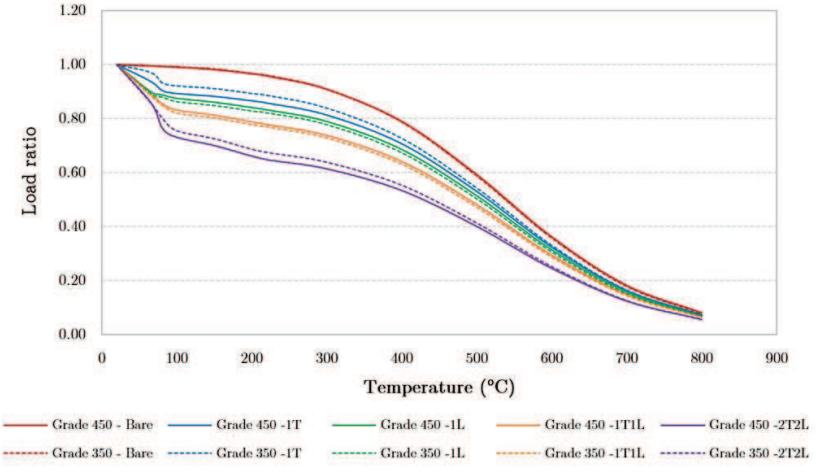

Figure 5. Reduction of axial compression capacity with temperature

Figure 5 presents the axial compression capacity expressed as load ratio versus exposed temperature curves obtained from the parametric study for 200x200x5 SHS sections only, where

the load ratio is defined as the ratio between the axial compression capacity at elevated temperature to that at ambient temperature. Other results are given in Imran (2018).

As expected, axial compression capacity is enhanced by CFRP strengthening at ambient temperature and increases with the number of CFRP layers. However, when temperatures exceed the glass transition temperature of the adhesive, the capacity reduces significantly and thus also the load ratio. The behavior of unstrengthened steel columns is independent of SHS sizes and steel grade. However, CFRP strengthened columns behave differently depending on CFRP strengthening configuration, SHS sizes and steel grade. CFRP strengthened columns with more CFRP layers exhibit a higher reduction in capacity since the higher capacity enhancement at ambient temperature is lost at elevated temperatures. Similar higher reductions are observed with high strength steel grades and slender SHS sections.

4 Fire Resistance Ratings of CFRP Strengthened SHS Columns

The results from experiments and FEA based parametric study showed that the axial compression capacities of CFRP strengthened steel columns reduced at elevated temperatures. Importantly, the critical failure temperature of CFRP strengthened steel columns is lower than that of unstrengthened steel columns at a given load ratio. Both test and FEA results showed the need to externally insulate and protect CFRP in order to achieve higher Fire Resistance Ratings (FRR) of steel columns under standard fire exposure. In this section, FRRs of CFRP strengthened and insulated SHS steel columns are predicted.

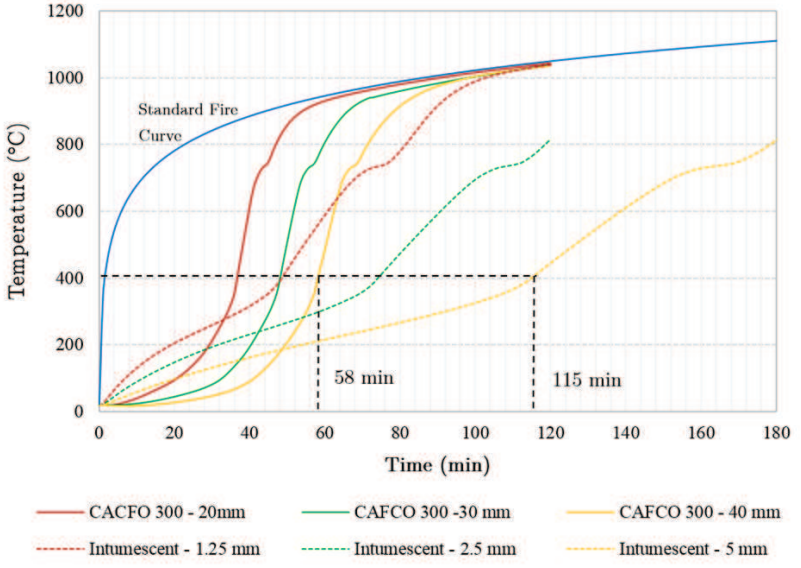

Figure 6. Time-temperature curves of steel column surface

For this purpose, the critical failure temperature, ie. the maximum steel temperature which a given column can withstand under a particular load ratio, was determined using the load ratio versus temperature curves obtained from the steady state FE analyses (Figure 5). They were similar for unstrengthened SHS columns for a given load ratio, but depend on SHS section sizes, steel grade and CFRP configuration for CFRP strengthened SHS columns. In the next step, time-temperature curves of steel surface when exposed to a standard fire were determined from a heat transfer analysis as described earlier. They are shown in Figure 6 for CFRP strengthened SHS steel columns with CAFCO300 external insulation of 20, 30 and 40 mm thicknesses. This

procedure was extended to cover intumescent paints of three thicknesses (1.25, 2.5 and 5 mm) in protecting CFRP strengthened SHS steel columns and their results are also shown in Figure 6.

In the final step, the structural failure time of column (FRR) was determined from the time-temperature curve of the steel surface (Figure 6) for a given critical failure temperature (Figure 5). The load ratio versus FRR/failure time curves were plotted for CFRP strengthened SHS columns insulated with CAFCO300 and intumescent paint. Figure 7 shows this plot for Grade 450 200x200x5 mm SHS columns and the other results are given in Imran (2018).

These load ratio-FRR curves can be used in the fire design of CFRP strengthened and insulated SHS columns. FRR increases with increasing insulation thickness while it reduces with higher number of CFRP layers. All the SHS columns considered in this study satisfy the 30 min FRR requirement when insulated with at least 30 mm of CAFCO300 insulation for load ratios up to 0.6. Five mm intumescent paint gives more than 2 hr FRRs for load ratios below 0.4 and 2.5 mm coating provides 30 min FRR for load ratios below 0.6.

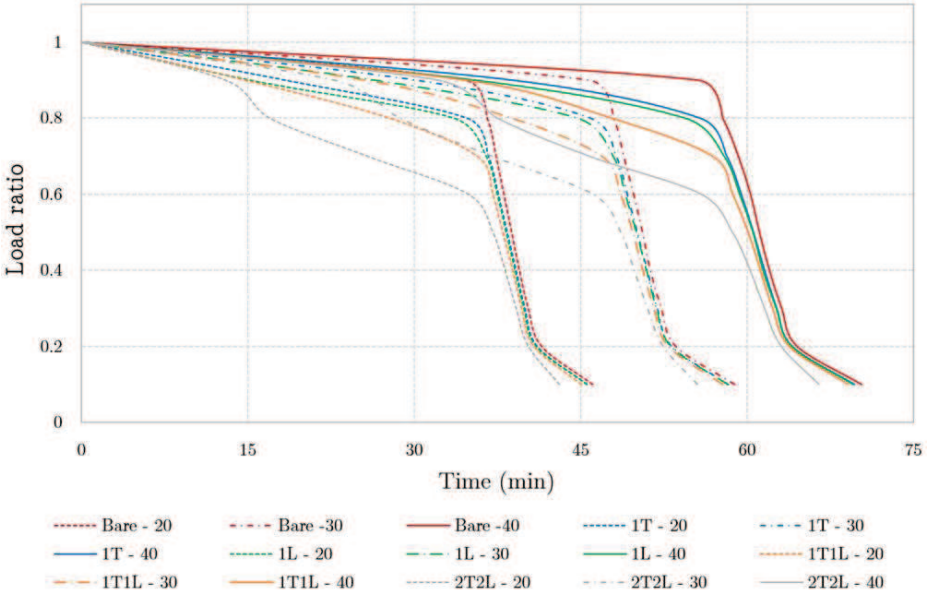

Figure 7. Load ratio-FRR curves of Grade 450 200×200×5 SHS columns with CAFCO300 insulation

5 Conclusions

Fire performance of CFRP strengthened short SHS steel columns with and without external insulation was investigated in this paper using finite element models validated using authors' experimental results. The behaviour of CFRP strengthened SHS steel columns exposed to uniform elevated temperatures was investigated using steady state FE models while transient state FE models were used for CFRP strengthened and externally insulated SHS columns under standard fire conditions. The axial compression capacity of CFRP strengthened SHS columns reduced significantly when the temperature exceeded the adhesive's glass transition temperature and thus demonstrated the need to use external insulation.

Fire resistance ratings (FRR) of CFRP strengthened SHS columns externally insulated with vermiculite and gypsum based CAFCO300 insulation and intumescent paint were determined using the load ratio-failure temperature curves obtained using steady state analyses and the time-temperature curves obtained using heat transfer analyses. FRR results showed that CFRP strengthened SHS steel columns can be designed to have satisfactory

FRR by using a suitable fire insulation system (insulation type and thickness). Fire engineers can choose a suitable insulation system to provide the required FRR from these results.

References

Shaat, A. and Fam, A., Axial loading tests on short and long hollow structural steel columns retrofitted using carbon fibre reinforced polymers, *Canadian Journal of Civil Engineering*, 33, 458-70, 2006.

Bambach, M. R., Jama, H. H. and Elchalakani, E., Axial capacity and design of thin-walled steel SHS strengthened with CFRP. *Thin-Walled Structures*, 47, 1112-21, 2009.

Imran, M., Mahendran, M. and Keerthan, P., Experimental and Numerical Studies of CFRP Strengthened Short SHS Steel Columns, *Engineering Structures*, 175, 879-94, 2018.

Imran, M., *Fire performance and design of CFRP strengthened and insulated cold-formed steel tubular columns*, PhD thesis, Queensland University of Technology, Brisbane, Australia, 2018.

Kodur, V. K. R., Bisby, L. A. and Green, M. F., Experimental evaluation of the fire behaviour of insulated fibre-reinforced-polymer-strengthened reinforced concrete columns, *Fire Safety Journal*, 41, 547-57, 2006.

Imran, M, Mahendran, M and Keerthan, P., Mechanical properties of cold-formed steel tubular sections at elevated temperatures, *Journal of Constructional Steel Research*, 143, 131-47, 2018.

De Lorenzis, L., Fernando, D. and Teng J. G., Coupled mixed-mode cohesive zone modeling of interfacial debonding in simply supported plated beams, *Int. J. of Solids and Structures,* 50(14-15), 2477-2494, 2013.

Teng, J. G., Fernando, D. and Yu, T., Finite element modelling of debonding failures in steel beams flexurally strengthened with CFRP laminates, *Engineering Structures*, 86, 213-24, 2015.

Alam, M. I., Fawzia, S. and Liu X. M., Effect of bond length on the behaviour of CFRP strengthened concrete-filled steel tubes under transverse impact, *Composite. Structures,* 132, 898-914, 2015.

Haszin, Z. Failure Criteria for Unidirectional Fibre Composites, *Journal of Applied Mechanics*, *Transactions ASME*, 47, 329-34, 1980.

Ferrier, E., Rabinovitch O. and Michel, L., Mechanical behavior of concrete-resin/adhesive-FRP structural assemblies under low and high temperatures, *Construction and Building Materials,* 127, 1017-1022, 2016.

Faggiani, A. and Falzon B. G., Predicting low-velocity impact damage on a stiffened composite panel, *Composites Part A*, 41(6), 737-749, 2010.

Nunes, F., Correia, J. R. and Silvestre N., Structural behavior of hybrid FRP pultruded beams: Experimental, numerical and analytical studies, *Thin-Walled Structures,* 106, 201-217, 2016.

Cree, D., Gamaniouk, T., Loong, M. L. and Green, M. F., Tensile and lap-splice shear strength properties of CFRP composites at high temperatures, *J. of Composites for Construction,* 19, 4014-4043, 2015.

Nguyen, T-C., Bai, Y., Zhao, X. L. and Al-Mahaidi, R. Mechanical characterization of steel/CFRP double strap joints at elevated temperatures, *Composite Structures*, 93:1604-1612, 2011